PAPER

Enhanced reduction of graphene oxide by means of charging and electric fields applied to hydroxyl groups

To cite this article: H Hakan Gürel and S Ciraci 2013 *J. Phys.: Condens. Matter* **25** 435304

IOP PUBLISHING JOURNAL OF PHYSICS: CONDENSED MATTER

J. Phys.: Condens. Matter **25** (2013) 435304 (10pp) doi:10.1088/0953-8984/25/43/435304

Enhanced reduction of graphene oxide by means of charging and electric fields applied to hydroxyl groups

H Hakan Gürel[1,2,3] **and S Ciraci**[1,2,4]

[1] UNAM-National Nanotechnology Research Center, Bilkent University, 06800 Ankara, Turkey
[2] Institute of Materials Science and Nanotechnology, Bilkent University, Ankara 06800, Turkey
[3] Technology Faculty, Department of Information Systems Engineering, Kocaeli University, Kocaeli 41380, Turkey
[4] Department of Physics, Bilkent University, Ankara 06800, Turkey

E-mail: ciraci@fen.bilkent.edu.tr

Received 28 June 2013, in final form 4 September 2013
Published 8 October 2013
Online at stacks.iop.org/JPhysCM/25/435304

Abstract

We present a first-principles study of the effects of charging and perpendicular electric fields on hydroxyl groups, both of which mediate the reduction of graphene oxide through the formation of H_2O and H_2O_2. Starting with an investigation of the interaction between the hydroxyl groups and graphene, we determine the equilibrium binding geometry, binding energy, and the diffusion path with a minimum energy barrier and show that those equilibrium properties are strongly affected by external agents. While co-adsorbed H and O form bound OH, co-adsorbed H and OH in close proximity form H_2O with almost no energy barrier. When negatively charged or subjected to a perpendicular electric field, the energy barrier between two OH co-adsorbed in close proximity is weakened or totally suppressed, forming an oxygen atom strongly bound at the bridge site, together with a water molecule. The water molecule by itself is very weakly bound to graphene and is prone to desorb from the surface, leading to the reduction of graphene oxide. It is therefore demonstrated that the reduction of graphene oxide is promoted to a large extent by negative charging or an applied perpendicular electric field, through the formation of weakly bound water molecules from hydroxyl groups.

(Some figures may appear in colour only in the online journal)

1. Introduction

Graphene oxide (GOX) is a critical material because it allows the production of large-scale graphene sheets through the reduction of oxidized multilayer graphene [1, 2]. Oxidized graphene can be obtained through oxidative exfoliation of graphite, which can be visualized as an individual sheet of graphene decorated with epoxy (C–O–C) and hydroxyl (C–OH) groups on both sides and edges. Several experimental and theoretical studies [1–17] attempting to clarify the character of the interaction of oxygen with graphene and the resulting oxidation/deoxidation reactions have concluded that these reactions, in fact, are rather complex and comprise the interplay of various molecules and atoms, such as O, O_2, OH, H, H_2O and CO, as well as external agents.

GOX has been also a subject of interest because the electronic properties of graphene, in particular its linear π and π^* bands [18], which cross at the Fermi level, undergo dramatic changes upon oxidation [19, 21–23]. Introducing a band gap, which varies with oxygen coverage and hence changes semimetallic graphene into a semiconductor, has been an active field of study in graphene-based nanoelectronics [23, 16]. It has been shown that one can write on oxidized graphene using the heated tip of a scanning tunneling microscope (STM), whereby the light reflecting (semiconducting) locations on the oxidized graphene become dark (metallic) after they are traced by the tip [22]. This

interesting result, leading to thermochemical nanolithography, is interpreted as the reduction (or deoxidation) of oxidized graphene and hence its metallization at the locations where the heated STM tip has traveled [22]. Furthermore, it has been reported that the oxidized surface of graphene can be changed reversibly between dark and light spots with an applied lateral electric field [23]. To tune the band gap, the extent of reduction can also be controlled by an applied perpendicular electric field, whereby deoxidized spots are produced underneath an STM tip under a specific bias [23]. These results indicate that the properties of graphene can be modified by the controlled and reversible reduction/oxidation of GOX, which can be realized by charging it or by applying a perpendicular electric field.

Interestingly, the formation energy related to the oxidation of graphene is negative; hence, graphene cannot be oxidized using oxygen molecules [16, 20]. Actually, O_2 is physisorbed to a bare graphene surface with a very weak binding energy [17]. Only at defect sites, such as holes and vacancies, can O_2 dissociate and its constituent oxygen atoms be adsorbed to carbon atoms having lower coordination numbers [20]. In contrast to O_2, the bonding of free oxygen to graphene is rather strong, and changes between 2.43 and 3.20 eV depending on the coverage [16]. The critical question to be addressed is why the desorption of oxygen and the resulting reduction can take place from GOX so easily in the presence of external agents despite the strong bond between oxygen and graphene.

Hydroxyl groups are anticipated to be a critical ingredient in controlling the reduction/oxidation of GOX and hence in monitoring its electronic properties. In particular, among other adsorbates, OH adsorbed to graphene has a relatively lower energy barrier for diffusion; hence, its reaction with other adsorbates is expected to be dominant. In this paper, we will consider hydroxyl groups and show that in the presence of external agents deoxidation of GOX can be readily realized through the formation of water molecules. As for the water molecules, they are weakly bound to graphene and prone to desorption from the surface. We first study the binding of H, H_2, OH and H_2O to graphene and their migration on graphene. We consider critical reaction paths involving H, OH and O, which are co-adsorbed in close proximity. Some of the reactions are exothermic and can take place almost spontaneously when the distance between the adsorbates becomes smaller than a threshold distance. Specific reaction paths can lead to the reduction of GOX, even if they need to overcome significant energy barriers. We show how these energy barriers can be modified by charging or by applying a perpendicular electric field to control oxygen desorption and hence the reduction process via hydroxyl groups. We find that the bonding of OH and the energy barrier between co-adsorbed OH, which hinder H_2O formation, are suppressed when GOX is negatively charged or subjected to a perpendicular electric field. In this respect, the present study is unique in revealing critical reaction paths in the reduction of GOX via hydroxyl groups.

2. Method

The scope of this study is to investigate the effects of an electric field and charging on OH that is adsorbed onto graphene. Here, we performed calculations for charged GOX by adding the desired amount of excess electrons for the case of negative charging or by removing electrons for the case of positive charging, where both cases are treated using periodic boundary conditions (PBC). Throughout the paper, $Q > 0$ (or surface charge density $\bar{\sigma} = Q/A$ in C m^{-2}, A being the area of the cell) indicates positive charging, namely the number of depleted electrons per cell; $Q < 0$ indicates negative charging, namely the number of excess electrons per cell, and $Q = 0$ signifies the neutral cell. The bare (super)cell is made up of $(n \times n)$ primitive unit cells of graphene; each supercell comprises $2n^2$ carbon atoms and $8n^2$ valence electrons. We assume that graphene planes, which repeat periodically along the z-axis, are parallel to the (x, y)-plane. The electric field $\vec{E}$, which is applied perpendicularly to the graphene plane, is specified as positive, i.e. $E_{\text{field}} > 0$, if it is along the z-direction (or is pointing towards the adsorbates, i.e. H, OH, O). This electric field induces electronic charge transfer from the adsorbate to graphene—and the case is vice versa if the direction of $\vec{E}$ is reversed, i.e. $E_{\text{field}} < 0$. Electric field induced charge transfer modifies the charge distribution, hence affecting the physical and chemical properties.

Developing appropriate formalisms to provide reliable predictions on the effects of charging and applied electric field have been the subject matter of several studies [17, 24–35]. The following conclusions have been arrived at regarding the features and limitations of first-principles methods in treating these external effects using plane wave (PW) and local basis (AO) sets: (i) when negatively charged, the electronic potential between periodically repeating graphene layers has a dip at the center of the vacuum spacing s. This dip forms a quantum well-like structure, with its depth from the Fermi level increasing both with s and with the excess charge $Q < 0$. (ii) PW calculations correctly predict charge spilling to the vacuum region for large s, which is the consequence of an artifact of PBC. (iii) On the other hand, such a spilling does not occur in AO calculations even if PBC are used, since local basis orbitals at carbon sites fail to represent states in the quantum well-like potential at the middle of the vacuum spacing. (iv) This is the artifact of AO calculations, which turned out to be its advantage, whereby the artifact of PBC is tacitly canceled out. (v) The electronic potential of one single graphene layer trapping the excess charge in the actual case is close to that obtained by AO calculations using PBC. Hence the results concerning charging and electric field obtained from AO calculations are expected to be very close to the results of the actual case—and are hence physical. (vi) This analysis can also be extended to graphene subjected to a perpendicular electric field $\vec{E}$. While the excess electrons can spill to the vacuum region at the lower energy side of the sawtooth-like electronic potential treated by PW and by using PBC, AO calculations provide predictions close to the actual case of single graphene under a perpendicular electric field $\vec{E}$.

In view of the above analysis concerning the artifact of the PW basis set using PBC, our results in this study

are obtained by performing first-principles spin polarized calculations within density functional theory (DFT) [36] using linear combination of numerical atomic orbitals (LCNAO). Therefore, the present results are expected to be very close to the results of the actual case corresponding to a single graphene layer under an electric field $\vec{E}$ or containing excess charge $Q < 0$.

We use a double ζ polarized basis set and the exchange–correlation functional is approximated by the Perdew, Burke and Ernzerhof (PBE) functional [37] within the generalized gradient approximation (GGA). A 200 Ryd mesh cut-off is chosen and the self-consistent field calculations are performed with a mixing rate of 0.1. The Brillouin zone is sampled with a Monkhorst–Pack mesh [38] with $(5 \times 5 \times 1)$ **k**-points, whereas we use $(45 \times 45 \times 1)$ **k**-points in specific systems. Core electrons are replaced by norm-conserving, nonlocal Troullier–Martins pseudopotentials [39]. Geometry optimization is performed by the conjugate gradient method, by allowing all the atomic positions and lattice constants to vary. Periodic boundary conditions (PBC) are used within the supercell geometry and the vacuum spacing between graphene layers in adjacent supercells is taken as 15 Å. The convergence for energy is chosen as 10^{-5} eV between two consecutive steps. In atomic relaxations, the total energy is minimized until the forces on the atoms are smaller than 0.04 eV Å^{-1}. Numerical calculations are carried out using the SIESTA package [40].

The binding energy, E_b, is calculated from the expression, $E_b = E_T[\text{graphene}] + E_T[\text{A/M}] - E_T[\text{A/M} + \text{graphene}]$, in terms of the total energies of the bare graphene supercell and of the free adatom = A or molecule = M (M = OH, H_2 and H_2O), and the structure optimized total energy of one *A* or one *M* adsorbed to each graphene supercell, respectively. All total energies are calculated in the same (4×4) supercell if it is not specified otherwise. $E_b > 0$ indicates a bonding structure.

3. Interaction of H_2O, OH and H with graphene

The interactions of H_2O, OH and H with graphene are essential for the reduction of GOX through desorption of H_2O and H_2O_2. Here we characterize their interactions in equilibrium conditions by calculating the optimized binding geometry, the corresponding binding energy, the minimum energy barrier in their diffusion and the path of diffusion with the lowest energy barrier.

3.1. Binding of H_2O to graphene

Water, an indispensable ingredient in the oxidation/reduction process of GOX, has chemical as well as van der Waals (vdW) interactions with graphene [41]. Since the generalized gradient approximation (GGA) does not include vdW interactions, it underestimates the binding energy between H_2O and graphene. The binding energy calculated using the GGA lies in the range 18–47 meV, depending on its orientation and position [42]. On the other hand, the local density approximation overestimates the binding energy to be 151 meV. Therefore, the binding energy of H_2O including the vdW interaction is estimated to be between 18 and 151 meV. It is really a weak interaction and a water molecule physisorbed to graphene can be desorbed near room temperature.

3.2. Binding of OH to graphene

It is demonstrated experimentally that OH is one of the critical functional groups existing in GOX [43, 44]. The binding energies and magnetic moments of OH adsorbed onto graphene are calculated for hollow (H), top (T) and bridge (B) sites on the graphene layer. As shown in figure 1(a), the top (T) site is most favorable energetically, with a binding energy $E_b = 0.97$ eV and a magnetic moment $\mu = 0.51\ \mu_B$. Carbon atoms underlying OH are displaced slightly upwards from the plane of the graphene. Earlier calculations found the binding energy of OH to be in the energy range between 0.54 and 0.86 eV [45–50]. The energy landscape shown in figure 1(b) is calculated by relaxing the position of all the carbon atoms, as well as the height z of a single adsorbed OH, while its x and y coordinates are fixed in the (4×4) supercell of graphene. These calculations are repeated for 36×36 (x, y)-grid points on a hexagon. One can deduce the minimum energy barrier to the diffusion to be $E_B = 0.49$ eV from the variation of the calculated total energies along the symmetry directions, T $\rightarrow$ H $\rightarrow$ B $\rightarrow$ T of the hexagon presented in figure 1(b). This comparatively low energy barrier allows easy migration of OH on graphene at elevated temperatures. We expect that E_B calculated at low coverage is modified at very high coverage due to an increase in hydroxyl–hydroxyl interactions [16, 51].

3.3. Binding of H and H_2 to graphene

The binding of atomic hydrogen H on graphene has been treated in earlier studies [52–54]. Binding energies reported by different authors vary in a wide range [55]. They lie between 0.47 and 1.44 eV, with the majority of data being between 0.6 and 0.85 eV. This variability can be ascribed to differences in the structures and the optimization procedure and computational methodology used to calculate the chemisorption of H on graphite [55]. Here, for the sake of completeness, we calculate the binding energy using the same calculation parameters and local basis set used throughout the present work. In agreement with previous studies, we found that the strongest binding of a H atom occurs at the top site, with a binding energy of $E_b = 0.76$ eV. The variation of the total energies of a H adatom moving along specific directions of the honeycomb structure are also calculated and the minimum energy barrier to the diffusion is found to be $E_B = 0.74$ eV, as shown in figure 1(c).

Similar to water molecules, the binding of hydrogen molecules, H_2, to graphene is weak. Calculations with the LDA VWN [56] functional result in a binding energy of 93 meV for molecular hydrogen. Due to the neglect of vdW interactions, GGA calculations using the PW91 and PBE functionals predict relatively lower binding energies of 23 meV and 13 meV, respectively [57].

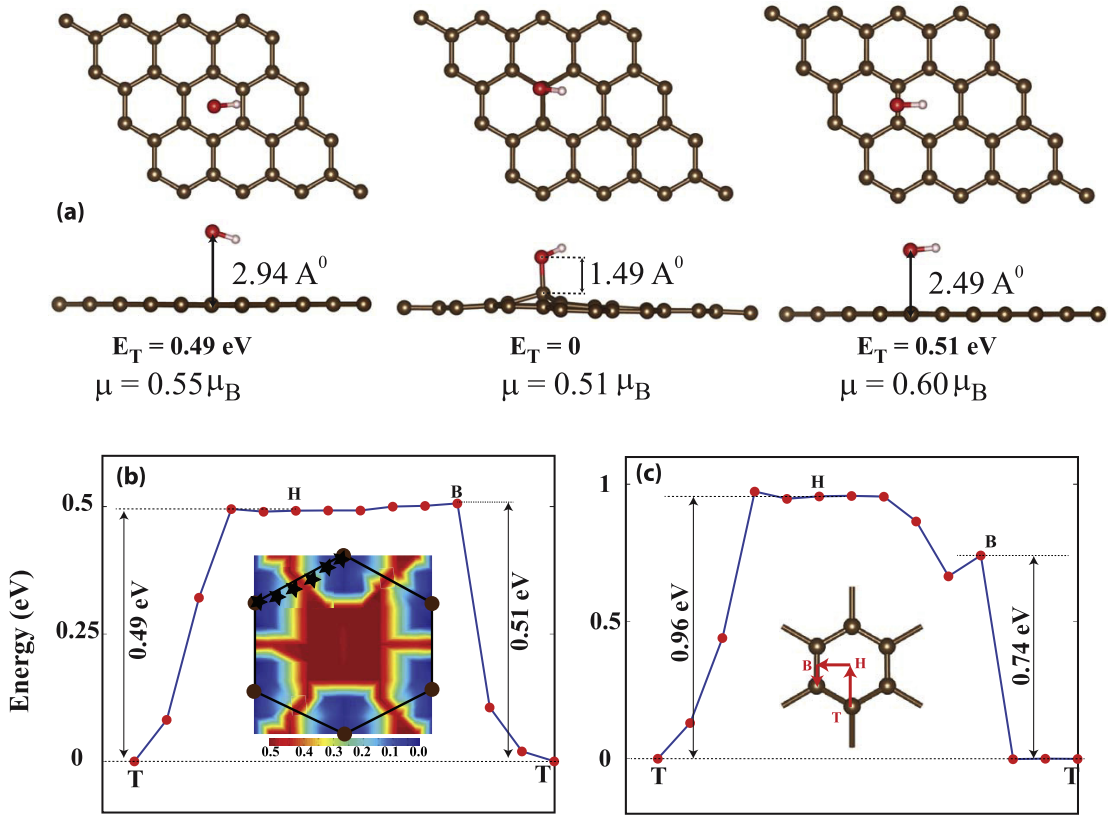

Figure 1. Interaction and bonding between OH/H and the graphene surface. (a) Top and side views of the atomic configurations, total energy E_T and magnetic moments μ in units of the Bohr magneton μ_B, of OH adsorbed onto hollow (H), top (T) and bridge (B) sites on graphene. The zero of energy is set to E_T at the top site. Large brown, large red and small yellow balls represent carbon, oxygen and hydrogen atoms, respectively. (b) The energy landscape of OH adsorbed onto different sites in the honeycomb structure and the variation of energy of OH migrating along the symmetry sites on a hexagon, i.e. T → H → B → T. The minimum energy barrier between T-sites and H-sites is $E_B = 0.49$ eV. A possible path for the minimum energy barrier for the diffusion of adsorbed OH is shown by stars. (c) The variation of energy of a H adatom migrating along the symmetry sites on a hexagon, i.e. T → H → B → T. The minimum energy barrier occurring between T-sites and B-sites is $E_B = 0.74$ eV. Accordingly, the H adatom migrates above the C–C bonds. Equilibrium binding energies of OH and H occur at the top site as 0.97 eV and 0.76 eV, respectively. Calculations are performed using a system where a single OH or H is adsorbed to each (4 × 4) supercell of graphene.

3.4. Effects of an electric field $\vec{E}$ and a charge Q on adsorbed OH

The effects of a perpendicular electric field $\vec{E}$ and a charge Q on OH adsorbed to graphene occur via the modification of the equilibrium charge distribution. In figure 2 we present the atomic geometry of adsorption, the isosurfaces of difference charge density, $\Delta\rho = \rho[\vec{E}\text{ or }Q] - \rho[\vec{E} = 0; Q = 0]$. For $E_{field} < 0$, electronic charge is transferred from the bottom site of graphene towards OH and the upper site leading to the accumulation of more charge on OH. The charge transfer is reversed when the direction of the perpendicular electric field is reversed, i.e. $E_{field} > 0$. Negative charging, $Q < 0$, realized by adding electrons in the system, gives rise to electron accumulation at OH, with electron depletion in the region between OH and the nearest carbon atom. This situation is, however, reversed for positive charging, $Q > 0$, realized by removing electrons from the OH + graphene system. Clearly, in the interaction of OH with graphene the strength of the bond is modified depending on the magnitude and direction of $\vec{E}$, as well as the sign and magnitude of charging.

In accordance with the above interaction and induced charge transfer/rearrangement, the internal geometric parameters of the OH–graphene bond, magnetic moment μ, and the effective charge on H and O atoms are affected by $\vec{E}$ and Q. As illustrated in figure 3, the bond length d of adsorbed OH increases with increased negative charging as well as with an increasing magnitude of negative E_{field}, but decreases with a relatively smaller rate with increased positive charging Q and an increasing magnitude of positive E_{field}. A larger bond distance implies the weakening of OH–graphene interactions, as we will clarify in the next paragraph. Similarly, the magnitude of the electronic charge on O and H atoms increases with increased negative charging, as well as with an increasing magnitude of negative $\vec{E}$. It appears that the bond strength decreases with increasing electronic charge on O. On the other hand, the angle θ between O–H and O–C bonds exhibits the opposite trend. The magnetic moment of a single OH adsorbed onto a supercell shows rather different behavior for Q and $\vec{E}$, as shown in figure 3. The magnetic state of neutral OH + graphene diminishes when $|Q| > 1$.

Among the effects discussed above, the effect of $\vec{E}$ and Q on the bond strength between OH and graphene has a

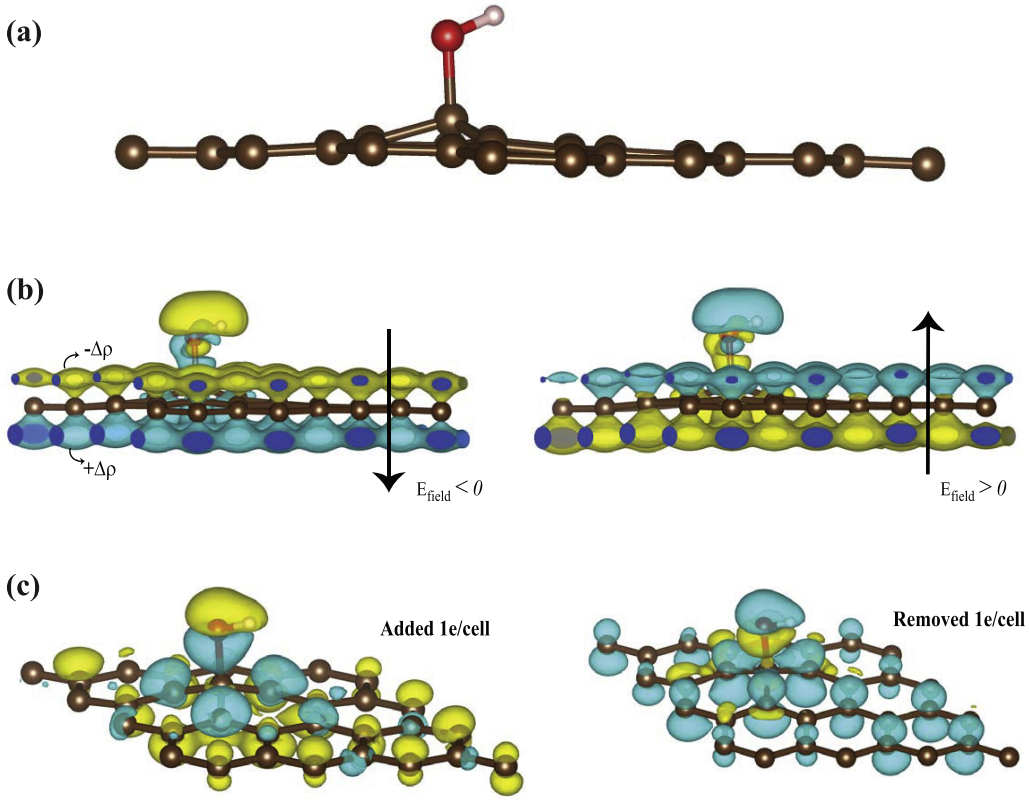

Figure 2. (a) Equilibrium atomic configuration of one OH adsorbed onto the top site of the (4 × 4) supercell of graphene. (b) Isosurfaces of the difference charge density $\Delta\rho$ under a perpendicular electric field $E_{\text{field}} = \pm 1.0$ V Å^{-1}. Negative and positive $\Delta\rho$ are shown by yellow and turquoise isosurfaces, respectively. (c) Isosurfaces of the difference charge density for $Q = \pm 1.0$ e/supercell.

bearing on the reduction of GOX. Here we further investigate the strength of the bond by calculating the optimized total energy of the OH + graphene system as OH is pulled in the perpendicular direction (z-direction) gradually for different values of Q (e per (4×4) cell) and for different values of E_{field}. For each fixed value Δz of OH from its equilibrium height, all carbon atoms in the supercell are relaxed, while carbon atoms at the corners of the supercell are fixed to prevent graphene from displacement. This analysis is continued by varying Δz. The variation of the total energies with pulling, Δz, are plotted in figures 4(b) and (c) for different values of Q and E_{field}, respectively. For the sake of comparison, we also included the pulling curves for $Q = 0$ and $\vec{E} = 0$. These figures convey interesting features regarding the effects of either Q or $\vec{E}$ on the strength of the OH–graphene bond. Normally, the energy associated with pulling $E_{\text{p}} = E_{\text{T}}[\text{OH} + \text{graphene}; Q, \vec{E}; \Delta z] - E_{\text{T}}[\text{OH} + \text{graphene}; Q, \vec{E}; \Delta z = 0]$ increases with increasing Δz, since the system is strained and pulled upwards. Eventually it passes through a maximum value denoted by E_{p}^{*} and drops suddenly at about $0.5 < \Delta z < 1.0$ Å. Our analysis suggests that E_{p}^{*} can be taken as a measure of the strength of the bond between OH and graphene. We note that E_{p}^{*}, namely the energy barrier to pull out the adsorbed OH from the graphene surface, is ∼1.3 eV for both $Q = 0$ and $\vec{E} = 0$. This energy is 0.33 eV larger than the equilibrium binding energy E_{b} of OH, since it corresponds to the strained configuration of underlying graphene, where carbon atoms at the corners of the supercell are fixed. An interesting feature of the present analysis is that E_{p}^{*} is strongly dependent on charging and the electric field. While E_{p}^{*} increases with $Q > 0$, it decreases dramatically for $Q < 0$. For example, $E_{\text{p}}^{*} \sim 1.8$ eV for $Q = +1.0$ e/cell, but it decreases to $E_{\text{p}}^{*} \sim 0.9$ eV for $Q = -1.0$ e/cell. Notably, for $Q < 0 E_{\text{p}}$ the curve does not exhibit a sharp fall on passing its maximum value. This is related to the excess charge on OH. Similarly, E_{p}^{*} can be as low as ∼0.35 eV under a perpendicular electric field $E_{\text{field}} = -1.0$ V Å^{-1}. We note that a bistability [17] may occur if OH moves in the reverse direction and hence approaches the graphene from $\Delta z > 1.2$ Å. These results clearly demonstrate that it is easier to desorb OH and achieve the reduction of GOX by negative charging or by applying an electric field $E_{\text{field}} < 0$. Under high local charging and a high local electric field, which can be attained by the sharp tip of a scanning tunneling microscope or by a gate voltage, the reduction of GOX can be easily achieved.

4. Desorption of oxygen from GOX

In the above sections we discussed the interaction of single H, H_2, H_2O and OH with the graphene surface and also revealed how the binding and related properties of OH are affected by an applied field $\vec{E}$ and the charge Q. The interactions of oxygen atoms with a graphene surface have been investigated thoroughly in earlier studies [16, 20, 17]. In this section we

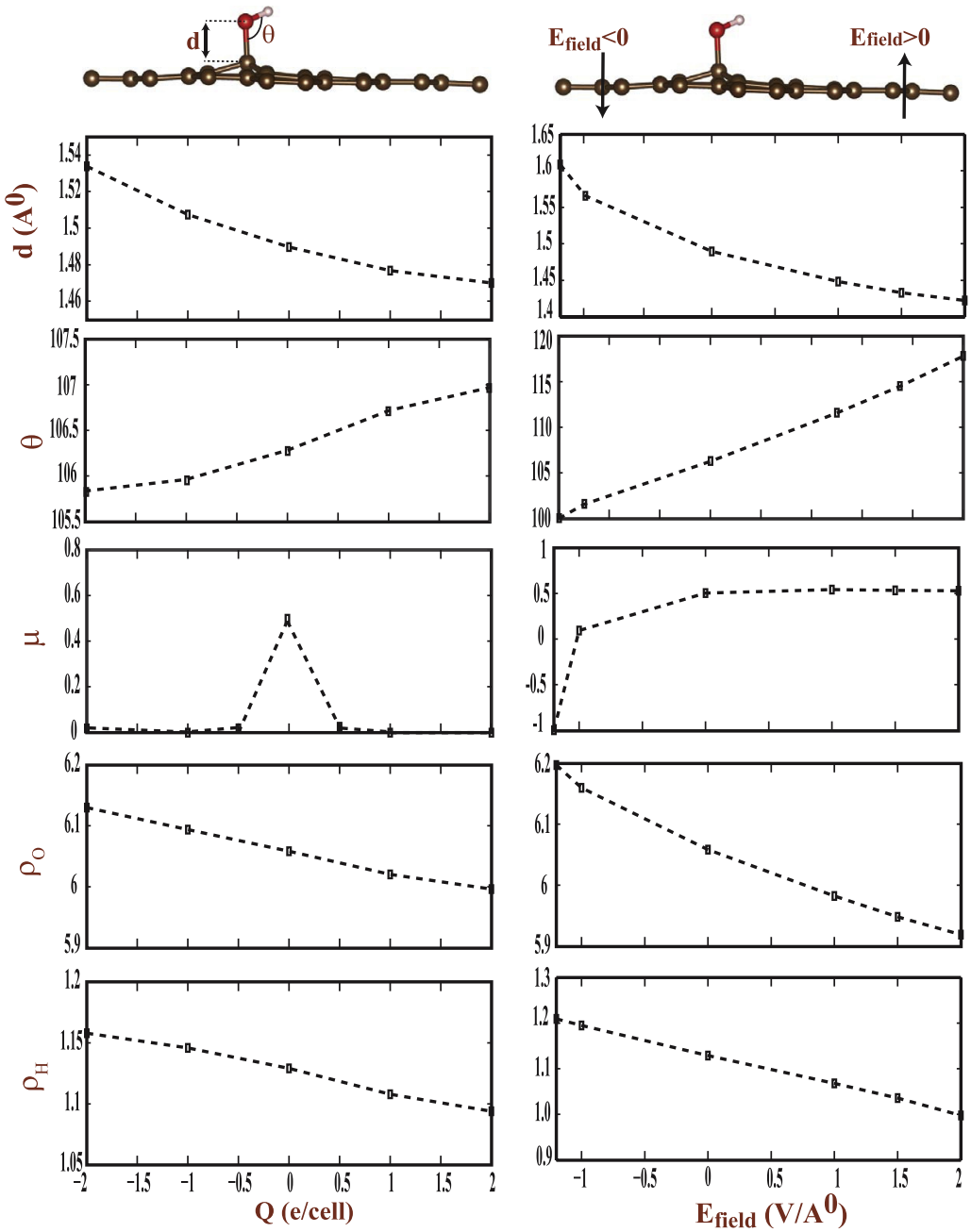

Figure 3. Variation of the bond length d of OH adsorbed onto graphene, the bond angle θ, the magnetic moment μ in units of the Bohr magneton μ_B, and the electronic charge on O and H atoms with charging Q and applied perpendicular electric field, $|\vec{E}|$. Calculations are performed using a (4 × 4) supercell.

investigate binary interactions among H, O and OH. Our objective is to reveal whether oxygen atoms can desorb from GOX via hydroxyl groups and how the reduction process is affected by Q and $\vec{E}$.

4.1. Interaction between adsorbed H and O atoms

We examine the interactions between co-adsorbed H and O atoms to see how OH can form. We consider three different paths for a H atom approaching the adsorbed O atom. (i) Both H and O are initially co-adsorbed; O is adsorbed at the bridge site and initially H is adsorbed at the top site in close proximity to the O adatom, as shown in figure 5(a). Here we move the adsorbed H atom on a migration path with the minimum energy barrier on graphene by fixing its x- and y-coordinates, but fully relaxing its z-coordinate, as well as all the coordinates of the adsorbed O atom and of all carbon atoms of graphene. As the co-adsorbed H approaches the adsorbed O, the energy falls suddenly by ∼1.4 eV when OH forms. This exothermic process occurs without any barrier. At this moment, owing to the constraints in the approach of H adatom, the O adatom desorbs to form a strong O–H bond. Eventually, OH becomes detached from the graphene. Apparently, the bond energy of OH compensates the binding

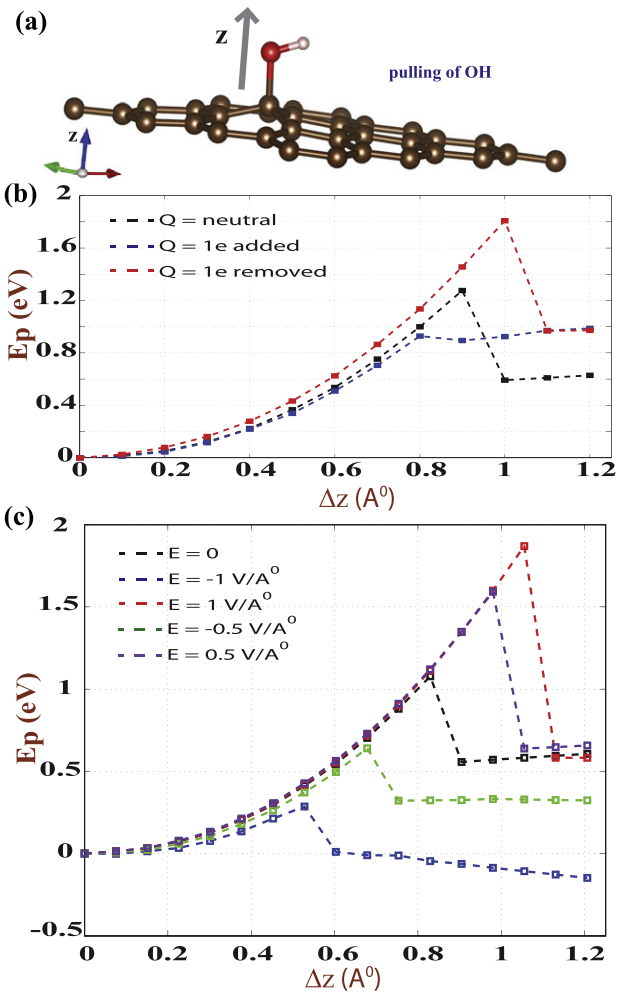

Figure 4. (a) Atomic configuration consisting of one OH adsorbed onto each (4 × 4) supercell of graphene, where OH is pulled in the perpendicular direction a distance Δz from its equilibrium height on the graphene surface. Large brown, large red and small yellow balls stand for C, O and H atoms, respectively. (b) The total energy E_p versus the distance Δz for different values of Q. (c) E_p versus the pulling distance Δz for different values of E_{field}. The zero of energy is set to the total energy corresponding to $\Delta z = 0$.

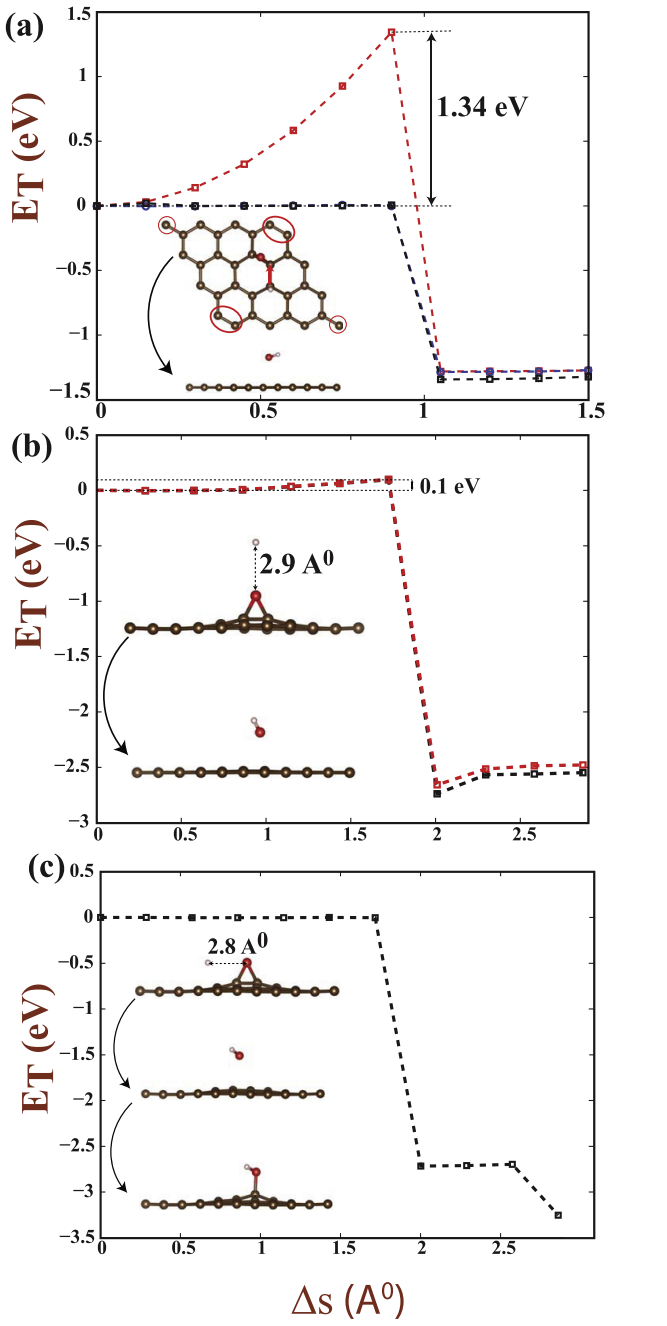

Figure 5. Variation of the total energy E_T as a H atom approaches the adsorbed oxygen from different directions with a displacement Δs. (a) The H adatom on graphene is approaching an oxygen atom adsorbed at the bridge site. The energy variation presented by black (red) dashed lines corresponds to a graphene substrate which is fully relaxed (fixed at the corner atoms). Δs follows the energy path with the minimum barrier described in the text. (b) A free H atom is approaching the adsorbed O atom vertically from the top and forms weakly bound OH. Here $\Delta s = -\Delta z$. (c) The H atom is approaching the adsorbed O atom horizontally. Weakly bound OH corresponds to an intermediate state, which is excited by ∼0.9 eV relative to the adsorbed OH. Calculations are performed using a (4 × 4) supercell of graphene. Large brown, large red and small yellow atoms are carbon, oxygen and hydrogen atoms, respectively.

energies of O and H atoms with graphene, as well as lowering the energy by ∼1.4 eV of the whole system. However, as shown in figure 5(a), an energy barrier of 1.3 eV can develop as the adsorbed H approaches the adsorbed O if the graphene is fixed from corner atoms rather than being fully relaxed. (ii) Along the second path shown in figure 5(b), where O is adsorbed at the bridge site, free H is approaching vertically from the top. At a specific distance overcoming an energy barrier of 0.1 eV, OH is formed in an exothermic process by lowering the energy of the system by 2.6 eV. Because of the strategy of the approach, the O adatom which is detached from graphene forms weakly bound OH. The gain of energy through the formation of free OH compensates the desorption of the O adatom. Upon the adsorption of OH the total energy can be further lowered to ∼3.3 eV. (iii) Along the third path shown in figure 5(c), whereby O is adsorbed, free H is approaching horizontally to form OH. The formation of OH occurs without any barrier, and the total energy is first lowered by 2.6 eV once weakly bound OH is formed. Thereafter, the energy is further lowered to ∼3.3 eV upon the adsorption of OH. It appears that the formation of OH through the

interaction between an O adatom and a H atom, which is either free in the environment or co-adsorbed to graphene, can occur easily with the release of significant energy. The formation of OH adsorbed on graphene is a crucial step towards the formation of H_2O from hydroxyl groups.

4.2. Interaction between H and OH adsorbed to graphene

Here we consider also three different cases to investigate the interaction between H and adsorbed OH. (i) As described in figure 6(a), initially one H and OH are co-adsorbed in close proximity and occupy the top sites of two outer carbon atoms of two adjacent C–C bonds. When a weakly bound H_2O is formed, the energy gained from this process compensates the sum of the binding energies of H and OH and further lowers the total energy by 2.65 eV. The cases shown in figures 6(b) and (c) are similar to the above analysis and involve the interaction between a free H atom and an adsorbed OH. In the case described in figure 6(b), the barrier is only 30 meV between the adsorbed OH and the free H atom. Once this small barrier is overcome, a weakly bound H_2O forms. In this exothermic process, an energy of 4.5 eV is released. This is a significant energy which can trigger other reactions. The reaction described in figure 6(c) takes place in two stages: first, a free H atom is bonded to graphene temporarily, and eventually an energy of 4.5 eV is released when a weakly bound H_2O is formed.

4.3. Interaction between two OH co-adsorbed in close proximity

Finally, we examine the interaction and chemical processes, when two OH co-adsorbed in close proximity approach each other. The interaction between two co-adsorbed OH is relevant for the deoxidation of GOX for the reasons pointed out at the beginning. Here, we move one OH along the path of the minimum energy barrier towards the other OH. While moving one OH, its x- and y-coordinates are fixed along the migration path, but its z-coordinate, all the coordinates of the second OH, as well as all the coordinates of the graphene atoms are fully relaxed. In this case, an energy barrier of ∼0.4 eV prevents these two OH from engaging in a chemical reaction. Note that due to OH–OH interaction this barrier is smaller than E_B in figure 1. When the energy barrier is overcome, the chemical reaction sets in to form one weakly bound H_2O molecule and one O atom bound to the bridge site. The former is prone to desorb easily and hence to remove one adsorbed O atom from GOX. The relevant processes, A → B → C, and the corresponding energy variation are shown in figure 7.

Since a significant barrier is involved in the OH–OH interaction, here we examine how the energy barrier at B is modified externally by charging or by applying an perpendicular electric field. First, we consider the case where the system is negatively charged by implanting two excess electrons, i.e. $Q = -2$ electrons/cell. Under these circumstances, the energy barrier is dramatically lowered to ∼0.1 eV. Overcoming this small barrier, configuration-A proceeds to configuration-D, whereby two co-adsorbed OH

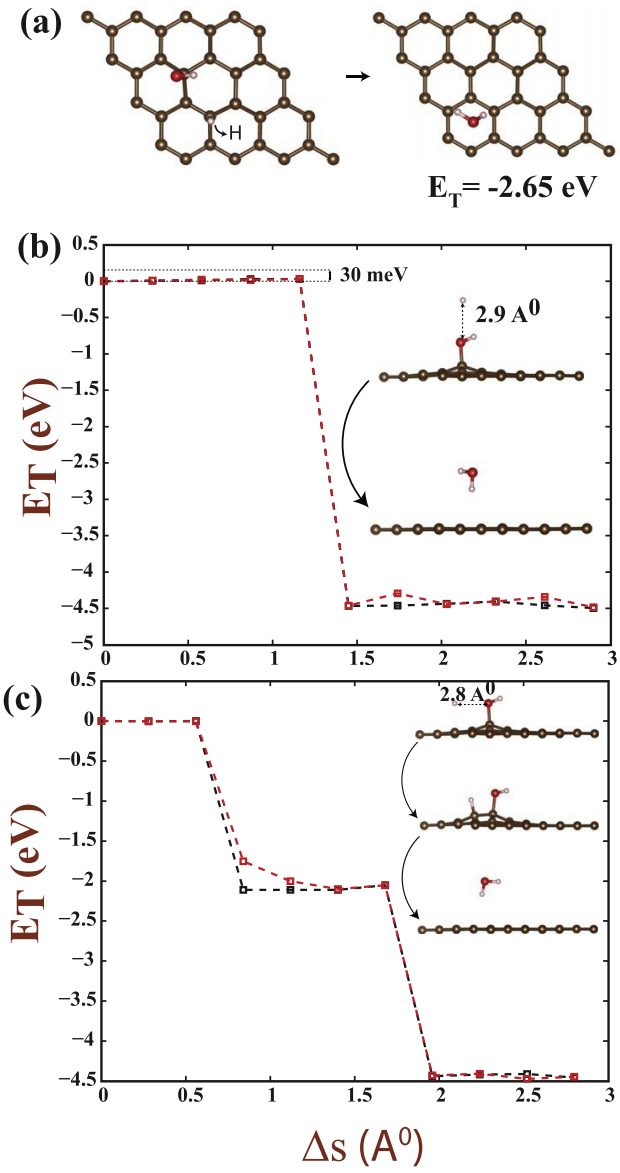

Figure 6. (a) Initially, H and OH are co-adsorbed and are in close proximity, occupying the outer top sites of two adjacent C–C bonds. When H_2O is formed the total energy is lowered by −2.65 eV. (b) Variation of the total energy E_T as a free H atom approaches OH from the top by $\Delta s = -\Delta z$. The formation of H_2O occurs upon overcoming an energy barrier of 30 meV. (c) As a free H atom approaches horizontally it is first adsorbed onto graphene and then forms H_2O. The whole process is exothermic and releases ∼4.5 eV. H_2O by itself is weakly bound to graphene and can desorb easily. Calculations are performed using a (4 × 4) supercell of graphene.

form one H_2O molecule and one O atom adsorbed to the top site. Interestingly, for $Q = -4$ electrons cell, the energy barrier completely disappears and the system passes directly from configuration-A to configuration-D, again forming weakly bound H_2O and an O atom adsorbed at the bridge site.

As shown in figure 7(b), the OH–OH interaction under an applied perpendicular $\vec{E}$ is reminiscent of the above charged cases. While the energy barrier of the neutral system under $E_{field} = 0$ corresponds to configuration-B, it increases to 0.95 eV under $E_{field} = +0.5$ V Å^{-1}. However, it decreases to 0.35 eV and to 0.05 eV under $E_{field} = -0.5$ V Å^{-1}

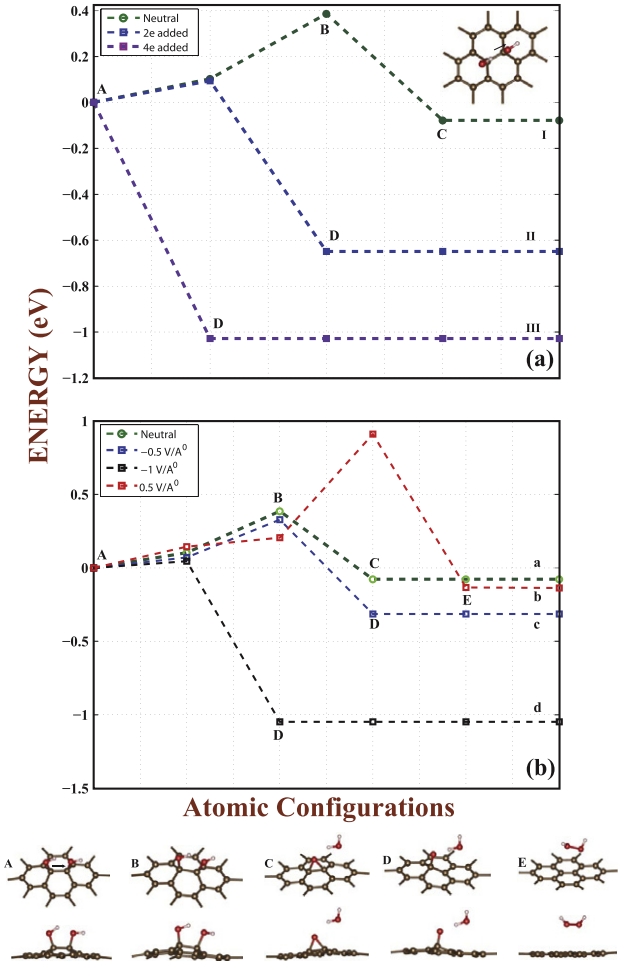

Figure 7. Variation of the total energy E_T as two OH adsorbed in close proximity approach each other. (a) The system is charged by $Q = -2$ and -4 electrons per supercell. (b) The system is under an electric field $E_{field} = +0.5$, -0.5 and -1.0 V Å^{-1}. The neutral system (i.e. $Q = 0$ and $E_{field} = 0$) is also shown by green dashed lines for the sake of comparison. Various atomic configurations, starting from A, going through B, and ending in C or D or E, are described at the bottom of the figure. Large brown, large red and small yellow balls represent C, O and H atoms, respectively. The zero of energy is set to the total energy of the initial configuration A, i.e. the two adsorbed OH are widely separated. Calculations are performed using a (6 × 6) supercell of graphene.

and $E_{field} = -1.0$ V Å^{-1}, respectively. Under $E_{field} = +0.5$ V Å^{-1}, the system transforms to configuration-E, whereby H_2O_2 is released.

The variation of the interaction energies of two co-adsorbed OH under an excess charge and/or a perpendicular electric field demonstrate the critical role played by hydroxyl groups in the reduction process of GOX. Since epoxy and hydroxyl groups coexist in GOX, desorption of oxygen adatoms can take place through H_2O or H_2O_2 almost spontaneously under an appropriate Q or $\vec{E}$.

5. Conclusions

The question of how graphene oxide can easily be deoxidized by charging or by applying an electric field in spite of the strong binding of single oxygen atoms to graphene has been extensively investigated. We considered interactions among co-adsorbed H, O, and OH. Adsorbed or free hydrogen atoms can easily interact with an oxygen adatom to form OH. Moreover, free or adsorbed hydrogen atoms can also interact with an adsorbed OH to form H_2O. Adsorbed OH by themselves can diffuse relatively easily and interact with each other. However, an energy barrier of 0.4 eV hinders them from engaging in a chemical process. We showed that by negatively charging the system or by applying a perpendicular field one can suppress this energy barrier and promote the chemical reaction to form H_2O. H_2O by itself is very weakly bound to graphene and can desorb at ambient temperatures. Each desorbed H_2O removes one oxygen atom from graphene oxide. Finally, we note that levels of charging or applied electric fields comparable to those used in this study can be achieved locally in experiments using the tip of an STM or femtosecond laser systems.

Acknowledgments

HHG acknowledges the support of TUBITAK-BIDEB. Part of the computational resources were provided by TUBITAK ULAKBIM, High Performance and Grid Computing Center (TR-Grid e-Infrastructure) and UYBHM at Istanbul Technical University through Grant No. 2-024-2007.

References

[1] Sniepp H C, Li J-L, McAllister M C, Sai H, Herrera-Alonso M, Adamson D H, Prud'homme R K, Car R, Saville D A and Aksay I A 2006 Functionalized single graphene sheets derived from splitting graphite oxide *J. Phys. Chem.* B **110** 8535–9

[2] Li J-L, Kudin K N, McAllister M J, Prudhomme R K, Aksay I A and Car R 2006 Oxygen-driven unzipping of graphitic materials *Phys. Rev. Lett.* **96** 176101

[3] Boukhvalov D W and Katsnelson M I 2008 Modeling of graphite oxide *J. Am. Chem. Soc.* **130** 10697–701

[4] Yan J, Xian L and Chou M Y 2009 Structural and electronic properties of oxidized graphene *Phys. Rev. Lett.* **103** 086802

[5] Yan J A and Chou M Y 2010 Oxidation functional groups on graphene: structural and electronic properties *Phys. Rev.* B **82** 125403

[6] Wang L, Sun Y Y, Lee K, West D, Chen Z F, Zhao J J and Zhang S B 2010 Stability of graphene oxide phases from first-principles calculations *Phys. Rev.* B **82** 161406

[7] Bagri A, Mattevi C, Acik M, Chabal Y J, Chhowalla M and Shenoy V B 2010 Structural evolution during the reduction of chemically derived graphene oxide *Nature Chem.* **2** 581–7

[8] Xiang H J, Wei S H and Gong X G 2010 Structural motifs in oxidized graphene: a genetic algorithm study based on density functional theory *Phys. Rev.* B **82** 035416

[9] Ghaderi N and Pressi M 2010 First principle study of hydroxyl functional groups on pristine, defected graphene and graphene epoxide *J. Phys. Chem.* **114** 21625–30

[10] Mattson E C *et al* 2011 Evidence of nanocrystalline semiconducting graphene monoxide during thermal reduction of graphene oxide in vacuum *ACS Nano* **5** 9710–7

[11] Pei S and Cheng H 2012 The reduction of graphene oxide *Carbon* **50** 3210–28

[12] Mao S, Pu H and Chen J 2012 Graphene oxide and its reduction: modeling and experimental progress *RSC Adv.* **2** 2643–62

[13] Huang H, Li Z, She J and Wang W 2012 Oxygen density dependent band gap of reduced graphene oxide *J. Appl. Phys.* **111** 054317

[14] Kim S, Zhou S, Hu Y, Acik M, Chabal Y J, Berger C, de Heer W, Bongiorno A and Riedo E 2012 Room-temperature metastability of multilayer graphene oxide films *Nature Mater.* **11** 544–9

[15] Sun T and Fabris S 2012 Mechanisms for oxidative unzipping and cutting of graphene *Nano Lett.* **12** 17–21

[16] Topsakal M and Ciraci S 2012 Domain formation on oxidized graphene *Phys. Rev.* B **86** 205402

[17] Topsakal M, Gurel H H and Ciraci S 2013 Effects of charging and electric field on graphene oxide *J. Phys. Chem.* C **117** 5943

[18] Novoselov K, Geim A, Morozov S, Jiang D, Zhang Y, Dubonos S, Grigorieva I and Firsov A 2004 Electric field effect in atomically thin carbon films *Science* **306** 666–9

[19] Dikin D A, Stankovich S, Zimney E J, Piner R, Dommett G H B, Evmenenko G, Nguyen S T and Ruoff R S 2007 Preparation and characterization of graphene oxide paper *Nature* **448** 457–60

[20] Topsakal M, Sahin H and Ciraci C 2012 Graphene coatings: an efficient protection from oxidation *Phys. Rev.* B **85** 155445

[21] Yao P P, Chen P L, Jiang L, Zhao H P, Zhu H F, Zhou D, Hu W P, Han B H and Liu M H 2010 Electric current induced reduction of graphene oxide and its application as gap electrodes in organic photoswitching devices *Adv. Mater.* **22** 5008

[22] Wei Z *et al* 2010 Nanoscale tunable reduction of graphene oxide for graphene electronics *Science* **328** 1373–137

[23] Ekiz O O, Urel M, Guner H, Mizrak A K and Dana A 2011 Reversible electrical reduction and oxidation of graphene oxide *ACS Nano* **5** 2475–82

[24] Poloni R, Miguel A S and Fernandez-Serra M V 2012 A first principles study of the effect of charge doping on the 1D polymerization of C_{60} *J. Phys.: Condens. Matter* **24** 095501

[25] Attaccalite C, Wirtz L, Lazzeri M, Mauri F and Rubio A 2010 Doped graphene as tunable electron–phonon coupling material *Nano Lett.* **10** 1172–6

[26] Aradi B, Hourahine B and Frauenheim T 2007 DFTB+, a sparse matrix-based implementation of the DFTB method *J. Phys. Chem.* A **111** 5678–84

[27] Bernard A S and Snook I K 2010 Transformation of graphene into graphane in the absence of hydrogen *Carbon* **48** 981–7

[28] Delley B 1990 An all-electron numerical method for solving the local density functional for polyatomic molecules *J. Chem. Phys.* **92** 508–17

[29] Ao Z M, Hernandez-Nieves A D, Peeters F M and Lia S 2012 The electric field as a novel switch for uptake/release of hydrogen for storage in nitrogen doped graphene *Phys. Chem. Chem. Phys.* **14** 1463–7

[30] Chan K T, Lee H and Cohen M L 2011 Gated adatoms on graphene studied with first-principles calculations *Phys. Rev.* B **83** 035405

[31] Brar V W *et al* 2011 Gate-controlled ionization and screening of cobalt adatoms on a graphene surface *Nature Phys.* **7** 43

[32] Suarez A M, Radovic L R, Bar-Ziv E and Sofo J O 2011 Gate voltage control of oxygen diffusion on graphene *Phys. Rev. Lett.* **106** 146802

[33] Makov G and Payne M C 1995 Periodic boundary conditions in *ab initio* calculations *Phys. Rev.* B **51** 4014–22

[34] Topsakal M and Ciraci S 2011 Static charging of graphene and graphite slabs *Appl. Phys. Lett.* **98** 131908

[35] Topsakal M and Ciraci S 2012 Effects of static charging and exfoliation of layered crystals *Phys. Rev.* B **85** 045121

[36] Hohenberg P and Kohn W 1964 Inhomogeneous electron gas *Phys. Rev.* **136** B864
Kohn W and Sham L J 1965 Self-consistent equations including exchange and correlation effects *Phys. Rev.* **140** A1133

[37] Perdew J P, Burke K and Ernzerhof M 1996 Generalized gradient approximation made simple *Phys. Rev. Lett.* **77** 3865–8

[38] Monkhorst H J and Pack J D 1976 Special points for Brillouin-zone integrations *Phys. Rev.* B **13** 5188

[39] Troullier N and Martins J L 1991 Efficient pseudopotentials for planewave calculations *Phys. Rev.* B **43** 1993

[40] Soler J M, Artacho E, Gale J D, Garcia A, Junquera J, Ordejon P and Sanchez-Portal D 2002 The SIESTA method for *ab initio* order-N materials simulation *J. Phys.: Condens. Matter* **14** 2745–79

[41] Lin X, Ni J and Fang C 2013 Adsorbtion capacity of H_2O, NH_3, CO, NO_2 on pristine graphene *J. Appl. Phys.* **113** 034306

[42] Leenaerts O, Partoens B and Peeters F M 2007 Adsorption of H_2O, NH_3, CO, NO_2, and NO on graphene: a first-principles study *Phys. Rev.* B **77** 125416

[43] Cai W W, Piner R D, Stadermann F J, Park S, Shaibat M A, Ishii Y, Yang D X, Velamakanni A, An S J and Stoller M 2008 Synthesis and solid-state NMR structural characterization of C-13-labeled graphite oxide *Science* **321** 1815–7

[44] Szabo T, Berkesi O, Forgo P, Josepovits K, Sanakis Y, Petridis D and Dekany I 2006 Evolution of surface functional groups in a series of progressively oxidized graphite oxides *Chem. Mater.* **18** 2740–9

[45] Jelea A, Marinelli F, Ferro Y, Allouche A and Brosset C 2004 Quantum study of hydrogen oxygen graphite interactions *Carbon* **42** 3189–98

[46] Lahaye R J W E, Jeong H K, Park C Y and Lee Y H 2009 Density functional theory study of graphite oxide for different oxidation levels *Phys. Rev.* B **79** 125435

[47] Kim M C, Hwang G S and Ruoff R S J 2009 Epoxide reduction with hydrazine on graphene: a first principles study *Chem. Phys.* **131** 064704

[48] Xu S C, Irle S, Musaev D G and Lin M C J 2007 Quantum chemical study of the dissociative adsorption of OH and H_2O on pristine and defective graphite (0001) surfaces: reaction mechanism and kinetics *Phys. Chem.* C **111** 1355–65

[49] Denis P A J 2009 Density functional investigation of thioepoxidated and thiolated graphene *Phys. Chem.* C **113** 5612–9

[50] Zhu Q, Lu Y H and Jiang J Z 2011 Stability and properties of two-dimensional graphene hydroxide *J. Phys. Chem. Lett.* **2** 1310–4

[51] Khantha H, Cordero N A, Molina L M, Alonso D A and Grifalco L A 2004 Interaction of lithium with graphene: an *ab initio* study *Phys. Rev.* B **70** 125422

[52] Jeloaica L and Sidis V 1999 DFT investigation of the adsorption of atomic hydrogen on a cluster-model graphite surface *Chem. Phys. Lett.* **300** 157

[53] Sha X and Jackson B 2002 First-principles study of the structural and energetic properties of H atoms on a graphite (0001) surface *Surf. Sci.* **496** 318

[54] Casolo S, Løvvik O M, Martinazzo R and Tantardini G F 2009 Understanding adsorption of hydrogen atoms on graphene *J. Chem. Phys.* **30** 054704

[55] Ivanovskaya V V, Zobelli A, Teillet-Billy D, Rougeau N, Sidis V and Briddon P R 2010 Hydrogen adsorption on graphene: a first principles study *Eur. Phys. J.* B **76** 481

[56] Vosko S H, Wilk L and Nusair M 1980 Accurate spin-dependent electron liquid correlation energies for local spin density calculations: a critical analysis *Can. J. Phys.* **58** 1200

[57] Henwood D and Carey J D 2007 *Ab initio* investigation of molecular hydrogen physisorbtion on graphene and carbon nanotubes *Phys. Rev.* B **75** 245413